

LARGE EDDY SIMULATION OF A METHANE TURBULENT DIFFUSION FLAME USING FLAME-SHEET APPROXIMATION

Araújo, H. F. S

University of São Paulo

Fukumasu, N. K.

University of São Paulo

Krieger Filho, G. C.

University of São Paulo

guenther@usp.br

Abstract. A numerical simulation of a methane turbulent diffusion flame using Large Eddy Simulation is carried out in the present work. The turbulence model is based on the Large Eddy method, where the large-scale flow is calculated directly and the subgrid-scale processes are modeled. In this method, the time-step of the simulation is set small enough to capture the characteristic time scale of the turbulence. The conservation equations are filtered so that only spatial mean values are available. Therefore, a model to the spatial averaged reaction rate, due the chemical reactions that take place in the molecular level, is need. In order to avoid the formulation of such spatial averaged reaction rate, as a first approach in the present work, the combustion processes is assumed to be described by the flame sheet approximation and the mixture fraction. No radiation losses are taken into account. The numerical method is based on finite volume method and the pressure-velocities coupling is done with the PRIME method. The time integration is based on the Euler method. The averaged conservation equations are written in cylindrical coordinates. The used subgrid approach is the Smagorinsky model. The investigated flame is a turbulent diffusion free jet flame burning methane. Experimental data of velocities, mixture fraction and temperature were taken from the International Workshop on Measurement and Computation of Turbulent Nonpremixed Flame. Averaged velocities and temperature are compared with the experimental data. Reasonable agreement is obtained for the velocities. By the temperature comparison, very large deviations are observed and are still under investigation

keywords: Combustion, Diffusion Flame, Large Eddies Simulation, Methane Flame

1. Introduction

The numerical simulation of combustion processes can be performed nowadays by the three classes of models: Direct Numerical Simulation (DNS), Large Eddy Simulation (LES) and Reynolds Averaged Navier-Stokes equations (RANS). The DNS needs no closure model to the Navier-Stokes equations but is not feasible for the simulation of engineering relevant flames due to the very large computing requirements. The limitations of the RANS methods are well documented in the literature. As a very promising method rises the LES method. In the LES the equations of motion are filtered so that the large scales of the turbulent motion are simulated whereas the smaller unresolved scales, smaller than the filter width, are modeled. The features of LES are twofold: on one hand the closure models are limited to the small scales of the turbulent flow and on the other hand, the computational time is practicable. Compared to RANS, LES is more computationally expensive but physically much more realistic. In the present work a nonpremixed turbulent methane flame is simulated with the LES method. A recent work simulating the same non-premixed turbulent methane flame has been done by R. Mustata and Bondi, 2006, using for the thermochemical model stocastic fields of the PDF transport equation. The presented results are very good. A very detailed reference on LES applied to nonpremixed turbulent flames is Kempf, 2003, where results for a turbulent non-premixed Hydrogen flame are presented. The turbulent thermochemical model used in the present work is based on the flame sheet model with the solution of the spatial averaged mixture fraction transport equation. The results are compared with the experimental data obtained from International Workshop on Measurement and Computation of Turbulent Nonpremixed Flame (TNF, 2006).

2. Mathematical formulation

Fluid motion can be described by a set of coupled partial differential equations. The main equations describe the transport of the conserved quantities and hence are known as conservation-equations. Assuming isothermal incompressible flow, the equations of conservation of mass and momentum (in all three spatial directions) adequately describe the flow. For reactive flows, additional transport-equations for the enthalpy and species concentrations must be considered. In LES a spatial filter is applied to the equations of motion and scalars. Doing this, only the large scale structures of the velocity and scalars fields are computed and the effects of the subgrid scales are modeled.

2.1. Filtering

The governing equations for a turbulent flame (continuity, momentum, species and energy) comprise the whole spectrum of length-scales. Therefore, the equations must be altered to purely resolve the large-scale features. This is done by low-pass filtering of the equations using a filter function h . This filter removes all the finer fluctuations, so that the governing equations only describe the space-averaged fields.

The filtered field $\overline{\Phi}(x_j, t)$ is determined by convolution with the filter-function $h(x_j - x'_j)$. As a result, the product of the local filter and the field Φ are averaged in space:

$$\overline{\Phi}(x_j, t) = \iiint_{-\infty}^{\infty} \Phi(x_j - x'_j) h(x'_j) dx'_1 dx'_2 dx'_3, \quad (1)$$

where x'_j refers to local coordinates, so $x'_j = 0$ at x_j .

The difference between the filtered field $\overline{\Phi}$ (large-scale portion of Φ) and the original field Φ is called its fine-structure or the small-scale portion Φ' .

$$\Phi - \overline{\Phi} = \Phi' \quad \Leftrightarrow \quad \Phi = \overline{\Phi} + \Phi' \quad (2)$$

A typical example for a filter function is the rectangle filter (top-hat filter) of the widths three Δ_j , which is defined by equation (3). In general, any low-pass filter can be chosen for LES, although only some make sense.

$$h(x_j - x'_j) = \begin{cases} \prod_{j=1}^3 1/\Delta_j & : |x'_j| \leq \frac{\Delta_j}{2} \\ 0 & : |x'_j| > \frac{\Delta_j}{2} \end{cases} \quad (3)$$

In turbulent reactive flows, there are density fluctuations, which originate unclosed terms that are difficult to model (Kempf, 2003). However, this can be avoided by applying density-weighted *Favre-filtering* instead. Favre filtering of a scalar Φ results in $\tilde{\Phi}$ and the fine-structure contribution Φ'' , which are defined in eq. (4). With Favre-filtering, a correlation $\overline{\rho\phi}$ is equal to $\tilde{\rho}\tilde{\Phi}$.

$$\tilde{\Phi} = \frac{\overline{\rho\Phi}}{\tilde{\rho}} \quad \text{with} \quad \Phi = \tilde{\Phi} + \Phi'' \quad (4)$$

In LES, a special filter is able to simplify the further proceeding: The *Schumann* filter is the top-hat filter on the base of the local mesh-cell, having the filter-widths Δ_j set equal to the size Δx_j of the local cell. This is the concept of *implicit* filtering (Kempf, 2003).

With Schumann-filtering, the integration interval in equation (1) can be narrowed to $-\Delta x_j/2 \leq x'_j \leq \Delta x_j/2$. With the substitutions $x_j^- = -\Delta x_j/2$ and $x_j^+ = \Delta x_j/2$, as well as the filter out of the integral, we obtain eq. 5. In this equation, the product in front of the integral is just the inverse volume of the local CFD-cell.

$$\overline{\Phi}(x_j, t) = \left(\prod_{k=1}^3 \frac{1}{\Delta x_k} \right) \int_{x_3^-}^{x_3^+} \int_{x_2^-}^{x_2^+} \int_{x_1^-}^{x_1^+} \Phi(x'_j, t) dx'_1 dx'_2 dx'_3 \quad (5)$$

In other words, Schumann-Filtering reduces the filtering process to volume-averaging over one cfd-cell, which happens anyway if finite volumes are applied.

2.2. Filtered Governing Equations

To obtain the LES equations, the governing equations must be filtered. After applying the filtering-operator, transformations are performed which are only valid if filtering- and derivation-operators commute, what is accepted as valid for the Schumann-Filtering.

2.2.1. Transport of Mass

Filtering equation of continuity yields the equation (6) for LES, which can be solved in filtered quantities just like the original equation:

$$\frac{\partial \bar{\varrho}}{\partial t} + \frac{\partial}{\partial x_j} (\overline{\varrho u_j}) = 0 \quad \Leftrightarrow \quad \frac{\partial \bar{\varrho}}{\partial t} + \frac{\partial}{\partial x_j} (\bar{\varrho} \tilde{u}_j) = 0 \quad (6)$$

2.2.2. Transport of Momentum

The same filtering technique is employed to the Navier-Stokes equations resulting:

$$\begin{aligned} \frac{\partial}{\partial t} (\bar{\varrho} \tilde{u}_i) + \frac{\partial}{\partial x_j} (\bar{\varrho} \tilde{u}_i \tilde{u}_j) = \\ \frac{\partial}{\partial x_j} \left[\bar{\varrho} \left(\nu \frac{\partial \tilde{u}_j}{\partial x_i} + \nu \frac{\partial \tilde{u}_i}{\partial x_j} \right) - \frac{2}{3} \bar{\varrho} \tilde{\nu} \frac{\partial \tilde{u}_k}{\partial x_k} \delta_{ij} \right] - \frac{\partial \bar{p}}{\partial x_i} + \bar{\varrho} g_i \end{aligned} \quad (7)$$

Equation (7) still includes unknown terms. With an negligible error, the diffusive term can be approximated by

$$\nu \frac{\partial \tilde{u}_j}{\partial x_i} \approx \tilde{\nu} \frac{\partial \tilde{u}_j}{\partial x_i} \quad (8)$$

and the correlation $\overline{\tilde{u}_i \tilde{u}_j}$ can be split up to the resolved part $\tilde{u}_i \tilde{u}_j$ and a fine-structure contribution τ_{ij}^{sgs} :

$$\overline{\tilde{u}_i \tilde{u}_j} = \tilde{u}_i \tilde{u}_j + \tau_{ij}^{\text{sgs}} \quad (9)$$

The fine-structure contribution τ_{ij}^{sgs} is known as *sub-grid stress* since it is representative of the shear stress due to the unresolved turbulent motion.

With (8) and (9), equation (7) can be altered to be solved in filtered quantities similarly to the unfiltered equation. The only difference is the addition of the sub-grid stresses to the diffusion term:

$$\begin{aligned} \frac{\partial}{\partial t} (\bar{\varrho} \tilde{u}_i) + \frac{\partial}{\partial x_j} (\bar{\varrho} \tilde{u}_i \tilde{u}_j) = \\ \frac{\partial}{\partial x_j} \left[\bar{\varrho} \tilde{\nu} \left(\frac{\partial \tilde{u}_j}{\partial x_i} + \frac{\partial \tilde{u}_i}{\partial x_j} \right) - \frac{2}{3} \bar{\varrho} \tilde{\nu} \frac{\partial \tilde{u}_k}{\partial x_k} \delta_{ij} + \bar{\varrho} \tau_{ij}^{\text{sgs}} \right] - \frac{\partial \bar{p}}{\partial x_i} + \bar{\varrho} g_i \end{aligned} \quad (10)$$

2.2.3. Transport of the Mixture-Fraction

The thermochemical model used in the present work is based on the conserved scalar formulation (Turns, 1996). In this framework, one has to solve the transport equation of the mixture fraction, which after the filtering reads:

$$\frac{\partial}{\partial t} (\overline{\varrho f}) + \frac{\partial}{\partial x_j} (\overline{\varrho f u_j}) = \frac{\partial}{\partial x_j} \left(\overline{\varrho D_f} \frac{\partial f}{\partial x_j} \right) \quad (11)$$

Here again, the convection term $\overline{\varrho f u_j}$ is split into its resolved part $\tilde{f} \tilde{u}_j$ and a fine-structure contribution F_j^{sgs} , which describes the flux due to unresolved turbulent motion:

$$\overline{\varrho f u_j} = \tilde{f} \tilde{u}_j + F_j^{\text{sgs}} \quad (12)$$

Using (12), equation (11) is modified to:

$$\frac{\partial}{\partial t} (\bar{\varrho} \tilde{f}) + \frac{\partial}{\partial x_j} (\bar{\varrho} \tilde{f} \tilde{u}_j) = \frac{\partial}{\partial x_j} \left(\bar{\varrho} \tilde{D}_f \frac{\partial \tilde{f}}{\partial x_j} + \bar{\varrho} F_j^{\text{sgs}} \right) \quad (13)$$

With the filtered governing equations for mass (6), momentum (10) and mixture-fraction (13), a set of coupled differential equations exists that describes the large-scale features of the flame investigated in this work.

2.3. Modeling the Sub-grid-Stresses τ_{ij}^{sgs}

In eq. (10), the sub-grid-stresses τ_{ij}^{sgs} represent the influence of the turbulent fine-structure u'_j on the resolved velocity field. Since the information on the small scales was removed by filtering, these terms can no longer be computed. However, they may be modeled as a function of known values.

2.3.1. The Eddy Viscosity Approach

The eddy-viscosity approach is based on the assumption that small-scale turbulence affects the flow in the same way as the molecular viscosity. Therefore, the fine-structure term τ_{ij}^{sgs} should be modeled by adding a turbulent viscosity ν_t to the molecular viscosity ν , resulting in an effective viscosity $\nu_{ef} = \tilde{\nu} + \nu_t$.

Adding the turbulent viscosity ν_t to model the sub-grid-stresses τ_{ij}^{sgs} in the filtered Navier-Stokes equations (10) corresponds to applying the following model:

$$\tau_{ij}^{\text{sgs}} = \nu_t \left(\frac{\partial \tilde{u}_j}{\partial x_i} + \frac{\partial \tilde{u}_i}{\partial x_j} \right) - \frac{2}{3} \nu_t \frac{\partial \tilde{u}_k}{\partial x_k} \delta_{ij} \quad (14)$$

However, this model would result in the trace of the stress-tensor τ_{ij}^{sgs} being zero. When using a pressure-correction scheme such as in this work, this constraint may be lifted by using the following model for the sub-grid-stresses:

$$\tau_{ij}^{\text{sgs}} - \frac{1}{3} \tau_{kk}^{\text{sgs}} \delta_{ij} = \nu_t \left(\frac{\partial \tilde{u}_j}{\partial x_i} + \frac{\partial \tilde{u}_i}{\partial x_j} \right) - \frac{2}{3} \nu_t \frac{\partial \tilde{u}_k}{\partial x_k} \delta_{ij} \quad (15)$$

With this approach, the trace elements of τ_{ij}^{sgs} remain unknown and the filtered Navier-Stokes equation (10) can be rewritten to yield:

$$\begin{aligned} \frac{\partial}{\partial t} (\bar{\rho} \tilde{u}_i) + \frac{\partial}{\partial x_j} (\bar{\rho} \tilde{u}_i \tilde{u}_j) = \\ \frac{\partial}{\partial x_j} \left[\bar{\rho} \nu_{ef} \left(\frac{\partial \tilde{u}_j}{\partial x_i} + \frac{\partial \tilde{u}_i}{\partial x_j} \right) - \frac{2}{3} \bar{\rho} \nu_{ef} \frac{\partial \tilde{u}_k}{\partial x_k} \delta_{ij} \right] - \frac{1}{3} \frac{\partial}{\partial x_i} \bar{\rho} \tau_{kk}^{\text{sgs}} + \frac{\partial \bar{p}}{\partial x_i} + \bar{\rho} g_i \end{aligned} \quad (16)$$

As mentioned previously, this work relies on a pressure correction scheme to determine the value of the pressure so that the equation of continuity is satisfied. This pressure correction is able to compute the sum of the pressure and the trace-term of the stress-tensor. Therefore, the pressure-parameter \bar{P} is introduced as shown in equation (17). The reader should be aware that solving equation (18) will only yield the pressure parameter \bar{P} , whilst the physical pressure \bar{p} remains unknown.

$$\bar{P} = \bar{p} - \frac{1}{3} \bar{\rho} \tau_{kk}^{\text{sgs}} \quad (17)$$

With the substitution given in eq. (17), the filtered momentum-equation (18) is obtained:

$$\begin{aligned} \frac{\partial}{\partial t} (\bar{\rho} \tilde{u}_i) + \frac{\partial}{\partial x_j} (\bar{\rho} \tilde{u}_i \tilde{u}_j) = \\ \frac{\partial}{\partial x_j} \left[\bar{\rho} \nu_{ef} \left(\frac{\partial \tilde{u}_j}{\partial x_i} + \frac{\partial \tilde{u}_i}{\partial x_j} \right) - \frac{2}{3} \bar{\rho} \nu_{ef} \frac{\partial \tilde{u}_k}{\partial x_k} \delta_{ij} \right] + \frac{\partial \bar{P}}{\partial x_i} + \bar{\rho} g_i \end{aligned} \quad (18)$$

2.3.2. The Smagorinsky Model

To solve the momentum-equation (18), a model providing an approximation for the turbulent viscosity ν_t is needed. As mentioned before, the model by Smagorinsky et al. (apud. Kempf, 2003) was used in this work.

The Smagorinsky model relates the eddy viscosity ν_t to the width Δ of the LES-filter and to the deformation-velocity-tensor \tilde{S}_{ij} :

$$\nu_t = (C_s \Delta)^2 \left| \frac{1}{2} \left(\frac{\partial \tilde{u}_j}{\partial x_i} + \frac{\partial \tilde{u}_i}{\partial x_j} \right) \right| \quad \text{or} \quad \nu_t = (C_s \Delta)^2 |\tilde{S}| \quad (19)$$

$$\text{with} \quad \tilde{S}_{ij} = \frac{1}{2} \left(\frac{\partial \tilde{u}_j}{\partial x_i} + \frac{\partial \tilde{u}_i}{\partial x_j} \right) \quad \text{and} \quad |\tilde{S}| = \sqrt{2 \tilde{S}_{lk} \tilde{S}_{lk}} \quad (20)$$

This model is based on a typical length-scale $C_s \Delta$ and a typical timescale (determined by the contraction of the deformation-velocity-tensor). The length-scale is chosen to be proportional to the local cell-width, which is coherent with the idea that only the unresolved structures (i. e. smaller than the cell-size) are to be modeled. In the present work, the value $C_s = 0.2$ was used.

2.4. Modeling the Turbulent Fluxes F_j^{sgs} of Mixture-Fraction

In the filtered mixture-fraction equation (11), the unknown term F_j^{sgs} must be modeled. Assuming once again that turbulence contributes to mixing like additional diffusion, F_j^{sgs} is approximated with an *eddy diffusivity* approach. This is similar to the *eddy viscosity* approach. With this approach, the structure of the transport equation (11) for the mixture-fraction remains similar to the non-filtered form. Herein, F_j^{sgs} is modeled by applying the “*turbulent diffusivity*” $D_{f,t}$ combined with the gradient of the filtered mixture-fraction $\partial\tilde{f}/\partial x_j$:

$$F_j^{\text{sgs}} = D_{f,t} \frac{\partial\tilde{f}}{\partial x_j} \quad (21)$$

With this model, the right hand side of equation (11) now reads:

$$\frac{\partial}{\partial x_j} \left(\bar{\varrho} \left(\tilde{D}_f + D_{f,t} \right) \frac{\partial\tilde{f}}{\partial x_j} \right) \quad (22)$$

The diffusion coefficients \tilde{D} and $D_{f,t}$ are proportional to the viscosities $\tilde{\nu}$ and ν_t and are only scaled by the Schmidt-Number σ . This describes the ratio of momentum transport due to viscosity to mixture-fraction transport due to diffusion:

$$\sigma = \frac{\nu}{D_f} \approx \frac{\tilde{\nu}}{\tilde{D}_f} \quad \text{and} \quad \sigma_t = \frac{\nu_t}{D_{f,t}} \quad (23)$$

We finally obtain the filtered and modeled equation for the mixture-fraction:

$$\frac{\partial}{\partial t} (\bar{\varrho}\tilde{f}) + \frac{\partial}{\partial x_j} (\bar{\varrho}\tilde{f}\tilde{u}_j) = \frac{\partial}{\partial x_j} \left(\bar{\varrho} \left(\frac{\nu_t}{\sigma_t} + \frac{\tilde{\nu}}{\sigma} \right) \frac{\partial\tilde{f}}{\partial x_j} \right) \quad (24)$$

The laminar Schmidt-number σ is formally accepted as 0.7 for air, whereas a wide range of turbulent Schmidt-numbers σ_t have been reported for the turbulent case.

2.5. Turbulent Thermochemical Model

A detailed description of methane combustion involves a large number of chemical species and reaction steps. The thermochemical model used in the present work is, however, very simple and based on the well-known flame sheet model (Turns, 1996). In the framework of the flame sheet model, reactions take place in a thin layer in the flame, where fuel and oxidator are present at stoichiometric ratio. Using the assumption that fuel and oxidator cannot co-exist, one is able to formulate algebraic relations between the mixture fraction and the mass fractions of fuel, oxidator and products (Turns, 1996). If, additionally, the flame is presumed to be adiabatic, then the enthalpy can be obtained in terms of the mixture fraction and thus the temperature and density can also be determined. The flame sheet has some severe shortcomings. In real flames, a high concentration of intermediate species (like OH, H or O radicals) exists in the (thin) flame-front. Since flame sheet neglects chemical kinetics, it cannot distinguish *reacting* from *reacted* gases. Hence, the concentration of intermediate species is neglected and the position of the flame-front remains unknown. Furthermore, the the flame sheet cannot describe effects like flame-quenching or re-ignition. Despite of all these shortcomings, the flame sheet model is deemed sufficient for the present purposes.

In LES, only the filtered value \tilde{f} of the mixture-fraction is known. To compute the dependent variables $\overline{\Phi(f)}$ (e. g. density or temperature), the sub-grid distribution of the mixture-fraction must be considered since Φ is generally a non-linear function of the mixture-fraction f . In order to do this several authors use a presumed PDF (probability density function) $p(f)$, which is a measure for the occurrence of a certain mixture-fraction. In the present work, however, a very crude approximation is used doing:

$$\overline{\Phi(f)} = \Phi(\tilde{f}) \quad (25)$$

In the future, the variance of the mixture fraction will be included in the calculations, so that a presumed β -function PDF will be constructed.

3. Test Case

In order to evaluate the proposed model, experimental data of a turbulent diffusion flame was used. The TNF D flame (TNF, 2006) is a piloted methane-air jet diffusion flame. The fuel consisting of 25 % methane and 75% air forms the inner fuel jet with a diameter of $D = 7.2$ mm. The flame is stabilized using a pilot

with a diameter of $D_p = 18.2$ mm. The pilot has a composition corresponding to that of a burnt fuel mixture. The central jet has a bulk velocity (U_0) of 49 m/s and the coflow velocity is 0.2 m/s. The bulk velocity of 49m/s leads to a fuel Reynolds number based on the nozzle diameter of $Re = 22400$. Experimental data of temperature and velocity were taken at the centerline of the jet.

4. Numerical Solution

The presented partial differential equations for mass, momentum and mixture fraction were solved using a finite volume based code. The convective terms are discretized in space with a hybrid method which switches from upwind to central difference schemes, depending upon the cell Peclet number. The pressure-velocity coupling is done using the PRIME method (Maliska, 1995). A explicit algorithm is used for time advance. The computational domain comprises a cylinder of $5D \times 60D \times 2\pi$ in radial, longitudinal and tangential directions, where D is the jet diameter. The used grid has $24 \times 100 \times 5$ nodes in the radial, longitudinal and tangential directions respectively. Convergence was achieved for each LES time-step after the residuals fall down to $1e-3$. A total of 5 flow-through time was used to collect the mean values presented in the next section. The flow-through time is defined herein as the time taken for a fluid particle on the centerline of the jet to travel through the domain.

5. Results

In this section the simulated mean values of axial velocity, mixture fraction and temperature are presented. All figures show the distribution of the variables along the centerline of the flame.

The centreline distribution of the mean axial velocity is depicted in Figure 1. One can see that the decay of the calculated velocity is overpredicted in comparison with the experimental data.

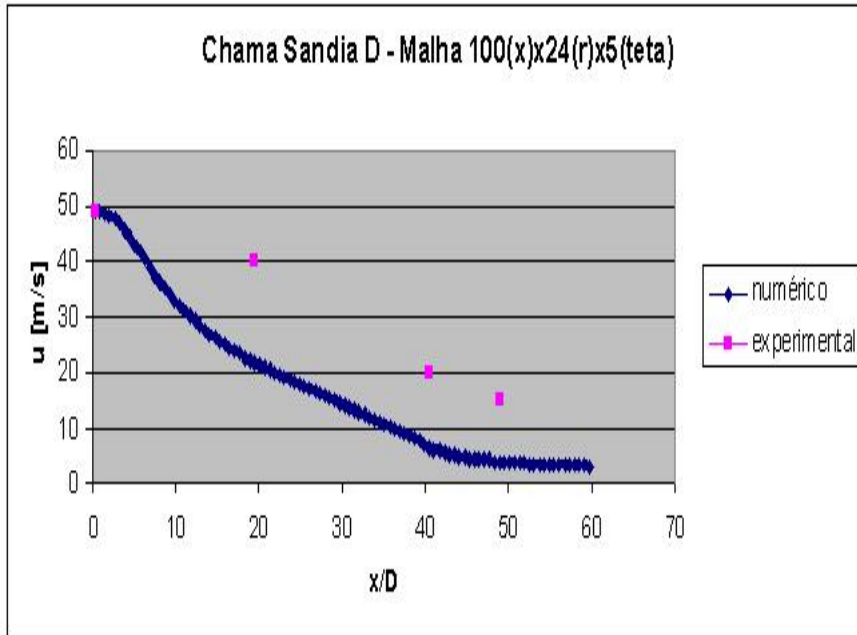


Figure 1: Mean axial velocity along the centerline. Line - simulation; dots experimental data

The centreline distribution of the mean mixture fraction is shown in Figure 2. Once again, one can see that the decay of the mixture fraction is overpredicted in comparison with the experimental data.

The centreline distribution of the mean temperature is shown in Figure 3. As a consequence of the mixture fraction, the temperature slope is too high in in comparison with the experimental data.

The distribution of the mean temperature shows a abrupt fall down at $x/D=40$, which is not verified at the experimental data. This is likely due the very crude aproximation, eq. (25), used for the sub-grid distribution of the mixture-fraction .

The simulation shows very large departure from the experimental data. These problems are still under investigation. Possible causes are the sub-grid model and grid dependence.

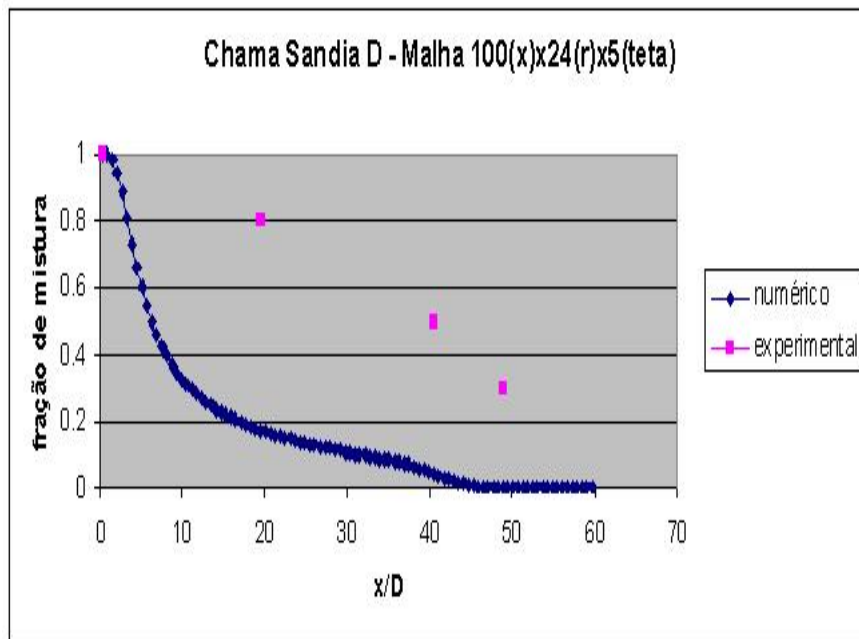


Figure 2: Mean mixture fraction along the centerline. Line - simulation; dots experimental data

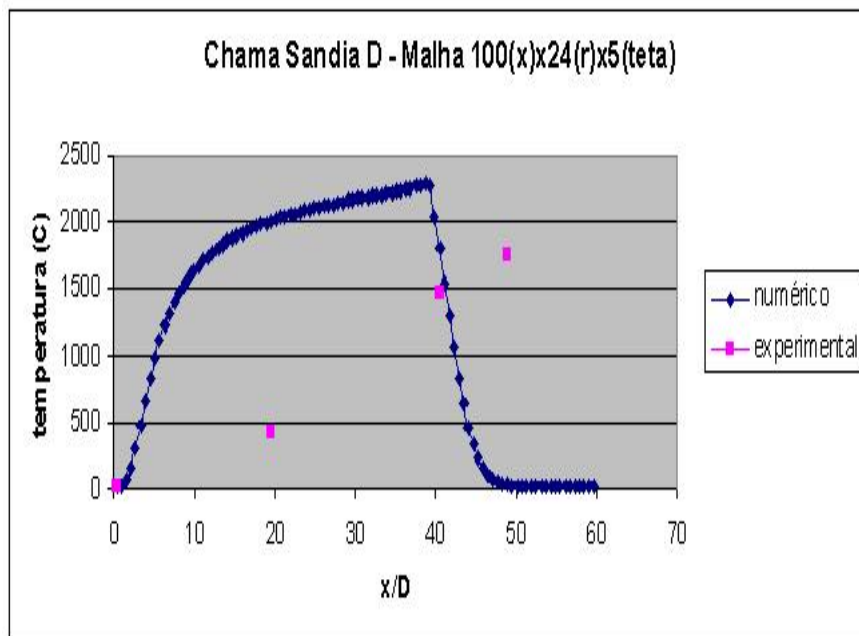


Figure 3: Mean temperature. Line - simulation; dots experimental data

6. Acknowledgements

The authors would like to thank FAPESP (São Paulo/Brazil) for supporting this project.

7. References

- Kempf, A. M., 2003, "Large Eddy Simulation of Non-Premixed Turbulent Flames", PhD thesis, Technische Universitaet Darmstadt, Germany.
- Maliska, C. R., 1995, "Transferência de Calor e Mecânica dos Fluidos Computacional", LTC Ed., Brazil.
- R. Mustata, L. Valiño, C. J. W. P. J. and Bondi, S., 2006, A probability density function Eulerian Monte Carlo field method for large eddy simulations: Application to a turbulent piloted methane/air diffusion flame (Sandia D), "Combustion and Flame", Vol. , No. 145, pp. 88–104.
- TNF, 2006, International Workshop on Measurement and Computation of Nonpremixed Flames.
- Turns, S. R., 1996, "An Introduction to Combustion - Concepts and Applications", McGraw-Hill.